RSC Advances




ROYAL SOCIETY OF CHEMISTRY

www.rsc.org/advances

# Nano silver-anchored reduced graphene oxide sheets for enhanced dielectric performance of polymer nanocomposites

S. Wageh[1], L. He[2], Ahmed A. Al-Ghamdi[1], Y.A. Al-Turki[3], S. C. Tjong[2]

[1]Department of Physics, Faculty of Science, King Abdulaziz University, Jeddah 21589, Saudi Arabia

[2]Department of Physics and Materials Science, City University of Hong Kong, Hong Kong

[3]Department of Electrical Engineering, Faculty of Engineering, King Abdulaziz University, Jeddah 21589, Saudi Arabia

Email: aptjong@cityu.edu.hk Tel.: (852) 34427702 Fax: (852) 34420538

*Abstract:* Nano silver-anchored reduced graphene oxide (Ag-RGO) was prepared and used as the filler material for polar polyvinylidene fluoride (PVDF) polymer. The percolation threshold of the Ag-RGO/PVDF composites was determined to be 1.52 vol.%. The results showed that the dielectric performance of the composite system was greatly improved by incorporating Ag-RGO sheets. The dielectric permittivity of the composite system reached a value of about 97 at 1 kHz, while maintaining a relatively low loss tangent. The enhanced dielectric performance of the composites was attributed to the presence of silver nanoparticles. These particles separated the RGO sheets from aggregation, thus increasing the interfacial areas within the composites greatly. When the composites were exposed to external electric

field, intense Maxwell−Wagner−Sillars polarization occurred at the interfacial areas. This led to enhanced dielectric permittivity of the composites. Coupled with low loss tangent and electrical conductivity, the Ag-RGO/PVDF composite system shows great promise for use as dielectric material for electronic capacitors.

*Keywords:* Graphene; Silver; Composite; Percolation; Dielectric permittivity;

## 1. Introduction

Polymer composites offer distinct advantages for technological applications including reduced weight, mechanical flexibility and ease of fabrication [1-4]. Polymer composites with high dielectric permittivity ($\varepsilon'$) show attractive applications for fabricating charge-storage capacitors of electronic devices [5]. Pure polymers generally have low dielectric permittivity of about 2-6. To enhance the dielectric permittivity, ceramic microparticles (e.g. barium titanate, lead zirconate titanate) with a large $\varepsilon'$ value are added to the polymers. However, large volume fractions of microparticles are needed to achieve desired dielectric properties. This leads to poor prcessability and inferior mechanical performance of resulting composites. Accordingly, conductive silver and nickel microparticles have been added to polymers for enhancing the dielectric performance [6, 7]. Such conductive filler additions result in a dramatic increase in $\varepsilon'$ near the percolation threshold. Dang et al. reported a large $\varepsilon'$ value of 400 at 1 kHz for the polyimide composite with 12.5 vol.% Ag content. By decreasing the size of silver particles to nanometer scale (40 nm), a filler loading of 22 vol.% is still needed to achieve percolation threshold with $\varepsilon' = 308$

[8].

The percolation threshold of conductive filler/polymer nanocomposites with a high dielectric permittivity can be reduced markedly by employing one-dimensional carbon nanotubes (CNTs) as nanofillers. CNTs with large aspect ratios enable the formation of a conductive network at low percolation threshold [9-12]. However, CNTs, especially single-walled CNTs are very expensive. Despite a large reduction in the price of multi-walled CNTs in recent years, their cost still remains relatively high [13]. Although a large increase in $\varepsilon'$ near the percolation threshold can be attained, CNT/polymer composites generally exhibit large dielectric loss (tanδ) due to the formation of a conductive path network.

Graphene, a monolayer of carbon atoms arranged into a two-dimensional honeycomb lattice, has attracted tremendous attention due to its excellent electrical, thermal, and mechanical properties [14–17]. Graphene exhibits large aspect ratio, exceptionally high mechanical strength, large electrical conductivity and high thermal conductivity. Thus, it is regarded as an ideal filler material for reinforcing polymers [18, 19]. It has been reported that graphene-based polymer nanocomposites exhibit much improved electrical and mechanical properties than the CNT/polymer composites [20, 21]. Graphene can be prepared in large scales by oxidizing graphite in strong acids, forming graphene oxide (GO). This is followed by reducing GO chemically/or thermally, producing chemically/thermally reduced graphene oxide (RGO) sheets. However, the strong van der Waals attraction force among the RGO sheets makes them hard to be dispersed homogeneously in the polymer matrix. Poor filler dispersion degrades the electrical properties of the resultant composites markedly. In this

study, we report the fabrication and characterization of the polymer composites with nanosilver-anchored RGO (Ag-RGO) sheets. Silver nanoparticles on the GO sheets serve as the spacers between them. Since the van der Waals force ($F$) between the RGO sheets drops rapidly with increasing distance ($d$), i.e., $F \sim d^{-6}$, silver decoration on the sheets are expected to sharply reduce the attractions. Furthermore, silver nanoparticles have been reported to be very effective fillers to improve the dielectric properties of the polymers [8, 22, 23]. Not all nanoparticles are effective to serve for these purposes. Oxide nanoparticles are obviously unsuitable due to their poor electrical conduction properties. For metal nanoparticles, only those with a high reduction potential capability are suitable. For those with a reduction potential more active (negative) than Ag, such as copper, cobalt, zinc, GO would be completely reduced to RGO and formed aggregation prior to the reduction of metal ions to nanoparticles and anchoring onto the RGO sheets. The polymer matrix material used is semi-crystalline polyvinylidene fluoride (PVDF). It has excellent electroactive properties, and found wide applications in electronic and biomedical engineering sectors [24]. To the best of our knowledge, this study presents the first report on the use of Ag-RGO sheets as a filler material to fabricate polymer composites with enhanced dielectric properties.

## 2. Experimental

Graphite flakes and PVDF (Kynar 500) were purchased from Sigma-Aldrich Inc. (U.S.A.) and Arkema Inc. (U.S.A.), respectively. Reagent grades chemicals such as silver nitrate, glucose, ammonia and *N, N*-dimethylformamide (DMF) were used as received. Graphite oxide was prepared by a typical Hummers method [25]. It can be readily exfoliated into

graphene oxide (GO) sheets. Atomic force microscope (AFM; Veeco Nanoscope V) examination reveals that the GO sheets are mostly a monolayer with a lateral dimension in the order of several micrometers (Figure 1).

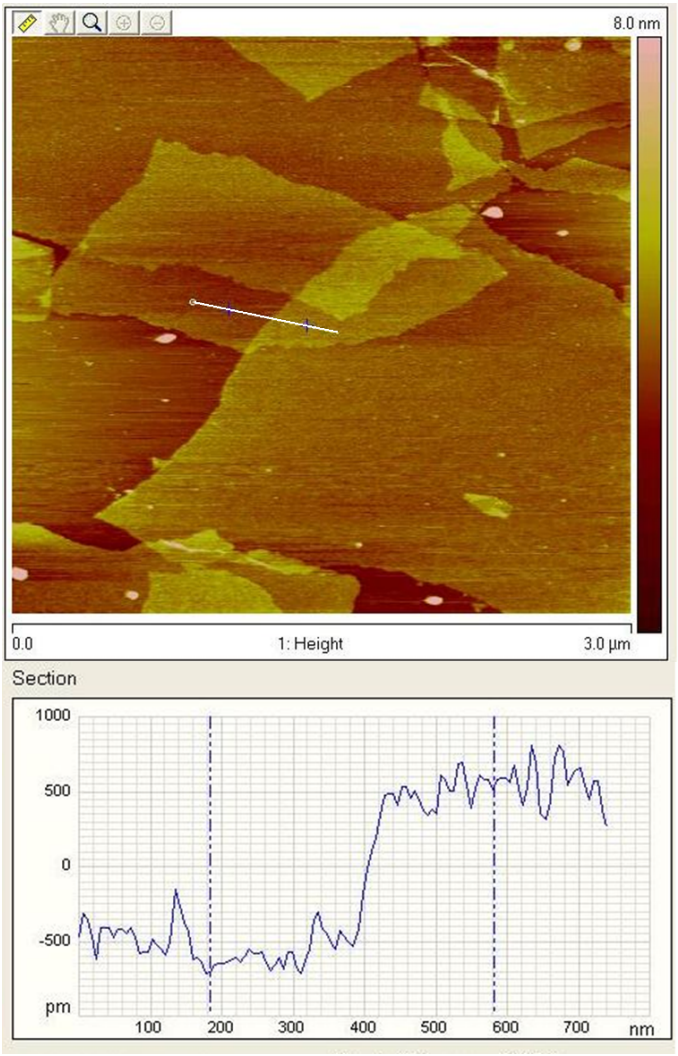


Figure 1 A typical AFM non-contact-mode image of GO sheets deposited onto a freshly cleaved mica. The superimposed cross-section measurement taken along the solid line indicates a thickness of about 1 nm.

Glucose was used to reduce silver ions and GO to yield Ag-RGO sheets. Typically, 15 mg

GO was dissolved in 15 ml distilled water to give a 1 mg/ml solution, then 0.4 g glucose was added to this solution. At the same time, 0.1 M ammonia solution was titrated to a certain amount of 0.1 M silver nitrate solution until the precipitate just disappeared. These two solutions were then mixed and stirred at 70 °C for 2 h. The mass ratios of GO to silver nitrate were kept at 1:1, 1:2 and 1:5. The black products were collected by centrifugation. Figure 2 shows the TEM micrographs of the Ag-RGO hybrid sheets. The hybrid sheets prepared with the GO/$AgNO_3$ ratio of 1:1 were selected as the fillers, since these sheets can be well dispersed in DMF. The formation of large amount *of Ag nanoparticles* resulted in the precipitation of hybrid sheet owing to an increase in the mass of RGO sheets, while small amounts of Ag decorations were not effective for inhibiting RGO aggregation. The Ag loading in RGO was estimated to be 60 vol.%, assuming $AgNO_3$ was fully converted to Ag, and the mass of RGO content was one-tenth of GO after reduction based on our previous TGA results [19].

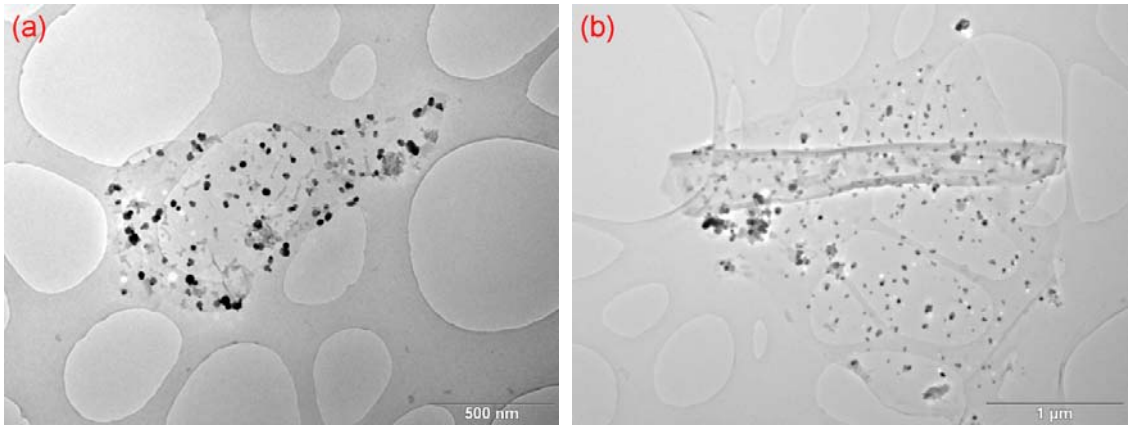

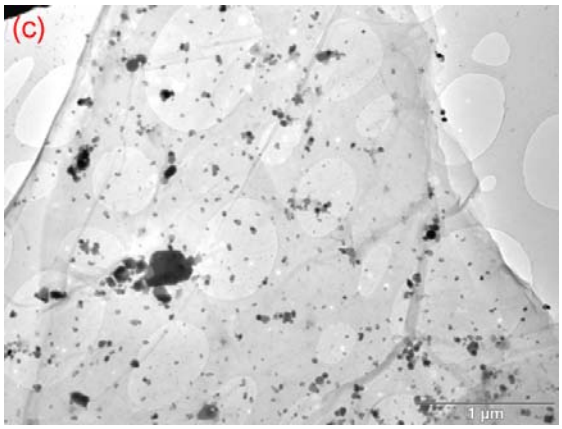


Figure 2 TEM micrographs of Ag-RGO sheets prepared with different GO/$AgNO_3$ mass ratios. (a) 1:1, (b) 1:2 and (c) 1:5.

The typical procedure of Ag-RGO/PVDF composite fabrication is shown in Figure 3. In the fabrication process, Ag-RGO composite sheets were re-dispersed in DMF under ultrasonication for 30 min. A certain amount of PVDF pellets were dissolved in DMF at 60 °C. These two solutions were then mixed and the obtained black solution was coagulated into a large amount of stirring water [26]. The Ag-RGO/PVDF composite mixture precipitated out immediately due to its insolubility in the DMF/water mixture. The obtained fibrous mixture was washed with distilled water and methanol, followed by drying at 60 °C overnight. Then the Ag-RGO/PVDF mixture was hot-pressed at 200 °C (at 50 MPa) into sheets of about 0.4 mm thick. After hot pressing process, it was found that a little amount of pores were produced, indicating a further thermal reduction of RGO. These pores were eliminated by a second hot-pressing cycle.

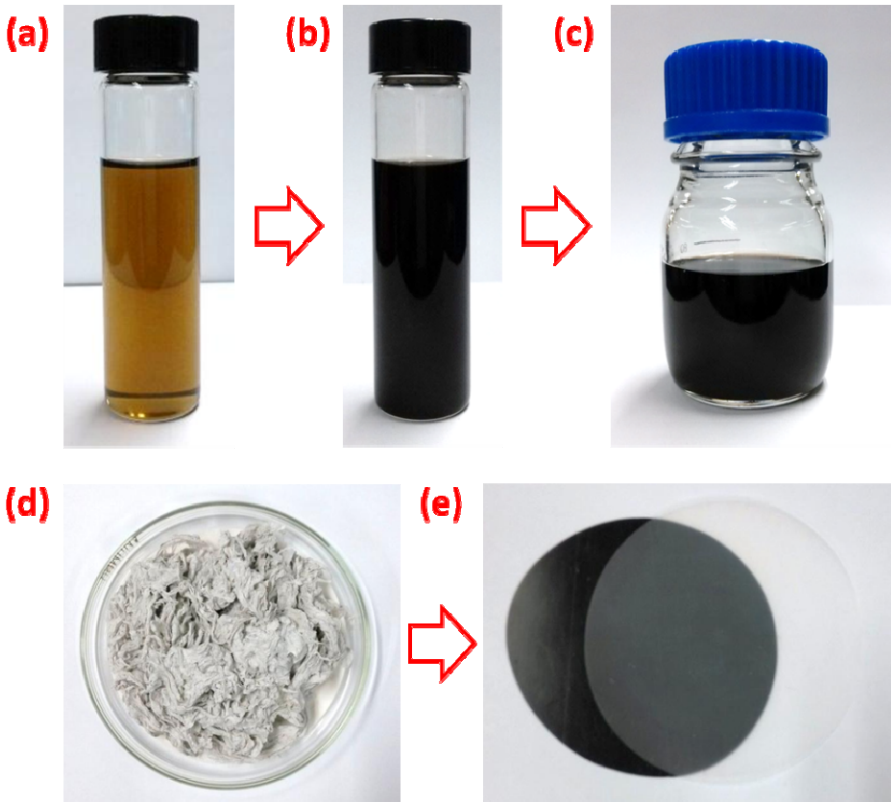


Figure 3 Fabrication route for the Ag-RGO/PVDF composites (a) Suspension of GO in water. (b) Suspension of Ag-RGO in DMF. (c) Suspension of Ag-RGO and dissolved PVDF in DMF. (d) Ag-RGO/PVDF composite mixture obtained through coagulation and vacuum filtration processes. (e) Hot-pressed Ag-RGO/PVDF composite sheet (1.5 vol.% filler content, left) and pure PVDF (right) of the same 0.4 mm thickness and processed in the same way.

The morphology of the Ag-RGO/PVDF composites was examined using a scanning electron microscope (SEM; Jeol JSM 820). The DC electrical conductivity of the composites was measured by a standard four-probe station. The dielectric properties and the AC electrical conductivity of these composites were measured by an Agilent 4284A Precision LCR Meter. For the electrical measurements, silver ink was painted on the specimen surfaces to form electrodes.

3. Results and Discussion

Figure 4(a) shows the electrical conductivity of the composites as a function of filler content. According to the percolation theory, a rapid increase in the electrical conductivity of composite materials takes place when the conductive filler forms an infinite network of connected paths through the insulating matrix. The conductivity of the composite $\sigma(p)$ above the percolation threshold ($p_c$) is given by [27, 28]:

$$\sigma(p) = \sigma_0(p - p_c)^t, \qquad \text{for } p > p_c. \tag{2}$$

where $p$ is the filler content and $t$ the critical exponent. Nonlinear fit in Figure 5(a) gives a $p_c$ value of 1.52 vol.% for the Ag-RGO/PVDF composites. Such a low $p_c$ is attributed to the large aspect ratio of the Ag-RGO sheets and their relatively homogeneous dispersion in the composite (Figure 4(b)). It is found that without the Ag decoration on the RGO sheets, the composite system displays percolation at about 2.51 vol.% as shown in Figure 5(a). The fitting results are listed in Table 1. It is considered that the Ag decoration on RGO sheets can improve the filler dispersion by inhibiting the attraction among the RGO sheets (Figure 4(b)). Without such decoration, the RGO sheets tend to form aggregates (Figure 4(c)).

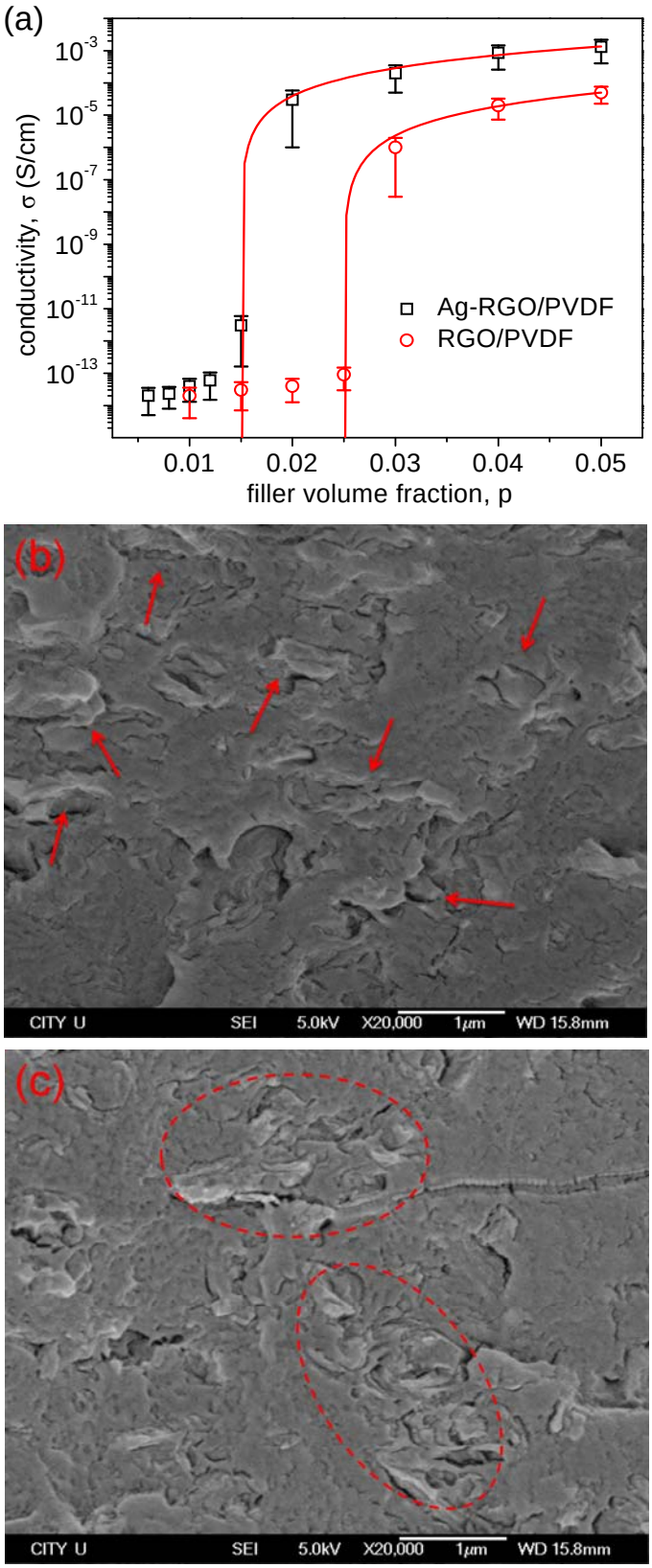


Figure 4 (a) Electrical conductivity of Ag-RGO/PVDF and RGO/PVDF composites as a

function of filler volume fraction. Solid lines are fitted curves using effective conductivity equation (Eqn. (2)). Fitted parameters are listed in Table 1. (b) and (c) are SEM micrographs of 2 vol.% Ag-RGO/PVDF and 2 vol.% RGO/PVDF composites, respectively. The Ag-RGO fillers are indicated with red arrows, and the RGO aggregations are indicated with dashed circles.

Table 1 Parameters characterizing the percolation behavior of Ag-RGO/PVDF and RGO/PVDF composites.

| Composite | $\sigma_0$ (S/cm) | $p_c$ | $t$ |
|---|---|---|---|
| Ag-RGO/PVDF | 0.59 | 1.52 vol.% | 1.82 |
| RGO/PVDF | 0.06 | 2.51 vol.% | 1.91 |

Figure 5 shows the dielectric performance of the RGO/PVDF and Ag-RGO/PVDF composites below $p_c$. Pure PVDF has a $\varepsilon'$ value of 7-8 at 1 kHz. When RGO was used as the fillers, the composite shows a sharp increase in the $\varepsilon'$ value near $p_c$. However, the dielectric loss also increases sharply (Figure 5(a)), which renders the material unsuitable for practical applications. It is rather difficult to control the RGO content to obtain a high $\varepsilon'$ value while at the same time not increase the dielectric loss. By contrast, the content of Ag-RGO hybrid fillers can be readily controlled to improve the dielectric performance of the resultant composites. Incorporation of 1.5 vol.% Ag-RGO into the PVDF would increase the $\varepsilon'$ about ten fold to 97, while at the same time maintain the dielectric loss at a relatively low level, as

shown in Figure 5(b). The improvement in $\varepsilon'$ can be attributed to the Maxwell−Wagner−Sillars (MWS) effect, which is commonly known as the interfacial polarization. MWS polarization occurs whenever there is an accumulation of charge carriers at an interface between two kinds of materials [29, 30]. As mentioned before, the Ag nanoparticles anchored on the RGO sheets separate the sheets apart, producing a large interfacial region within the composite. Since the electrical charges in conductive Ag-RGO are delocalized, they can be driven by the applied electric field, therefore accumulate at the Ag-RGO/PVDF interface, which contribute to the polarization effect. As the Ag-RGO content increases, the interfacial region increases rapidly and the MWS polarization improves significantly. As a result, the dielectric permittivity of the composite increases with filler content. Although percolated Ag-RGO/PVDF composites ($p > p_c$) may exhibit even higher $\varepsilon'$ values, the high dielectric loss of those composites precludes their practical applications in capacitors. The dielectric loss relates to the energy dissipation in a dielectric material through electrical conduction (transport-related loss), slow polarization currents (dipolar loss), and other dissipative phenomena such as interfacial polarization contribution. For Ag-RGO/PVDF composites with $p < p_c$, it is found that the dielectric loss maintains at a low level, even for near percolated composite ($\tan\delta = 0.29$ at 1 kHz, for $p = 1.5$ vol.%), as shown in Fig. 5(b)). At low filler content ($p \leq 1.1$ vol.%), it drops to below 0.05, demonstrating that for such material the energy loss can almost be neglected.

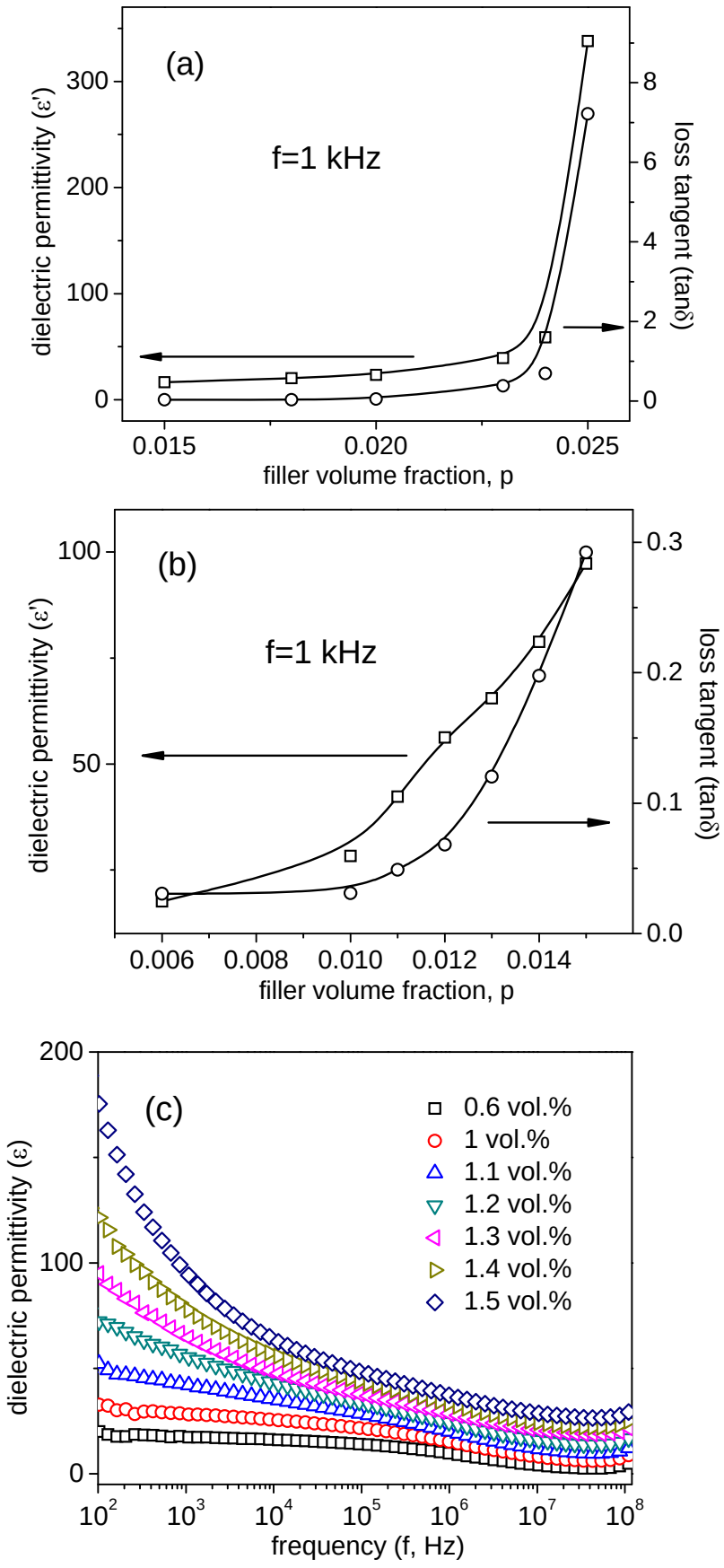

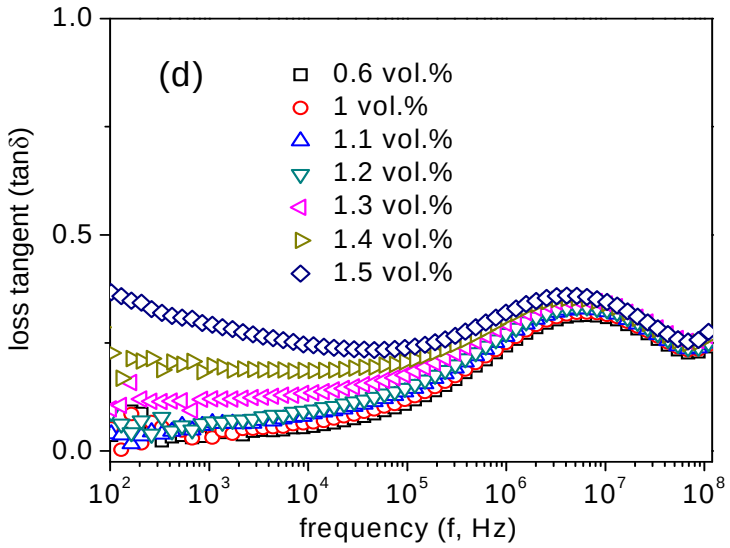


Figure 5 Effect of (a) RGO and (b) Ag-RGO volume fraction on dielectric permittivity and loss tangent of the composites. (c) Frequency-dependent dielectric permittivity and (d) loss tangent vs frequency of Ag-RGO/PVDF composites with various filler contents.

The frequency dependency of the dielectric permittivity and loss tangent of Ag-RGO/PVDF composite was depicted in Figure 5(c)-(d). All composite samples exhibit a similar tendency in their variation of dielectric properties against the testing frequency. At low filler content, the $\varepsilon'$ is nearly independent of frequency. With increasing filler content the frequency dependency gradually becomes pronounced. It can be found that the dielectric permittivity of the sample with high a filler loading ($p$ = 1.5 vol.%) decreases markedly from low to high frequency. This is mainly due to the fact that the MWS polarization can not contribute as much to the high frequency dielectric permittivity as it can do to the low frequency dielectric permittivity. Since the MWS polarization relates to the charging-discharging of the interfacial region within the composite, at higher frequency the charging-discharging cycle can not be finished completely. Thus its contribution to dielectric

response drops accordingly. In addition, the polymer matrix also plays its roles. Below 100 kHz, the dielectric response of the PVDF-based fluoropolymers is associated with both the dipoles alignment in the amorphous phase and the weak swing of dipoles in the microcrystal grains [31]. As the frequency increases, the contribution of the crystal phase diminishes. This also leads to a decrease in dielectric permittivity.

Figure 5(d) shows that for samples with higher filler content ($p \geq 1.4$ vol.%), the tanδ decreases with the frequency at low frequency range and increases with the frequency at high frequency range. It is generally believed that the high-frequency process is mainly associated with dipolar relaxation. The relaxation peak was reported to have two random molecular motions, including the micro-Brownian motion of the noncrystalline molecular chains ($\beta$-relaxation) and the motion of the molecular chains onto the amorphous/crystalline interfaces [32, 33]. At lower frequencies, the contributions of MWS polarization and electrical conduction are significant [34]. Since the MWS polarization is dominant and it decreases at higher frequency, the tanδ drops accordingly. For samples with lower filler content ($p \leq 1.3$ vol.%), the low frequency dependency of the tanδ is not particularly pronounced, implying that the contribution of MWS polarization to dielectric loss diminishes at low filler content. In this regard, the other effects (usually the dipolar loss) are primarily responsible for the dielectric loss.

From the literature, other researchers have also reported the use of graphene derivatives as the filler materials for enhancing the dielectric performance of the polymers. Using

chlorinated RGO sheets as the fillers ($p$ = 0.1 wt.%), Kim et al obtained $\varepsilon'$ value of ~90 and a low tanδ of ~0.04 at 1 kHz for the RGO/cyanoethyl pullulan composites [35]. Dimiev et al. reported that the 2 wt.% graphene nanoribbons loading improves dielectric permittivity of silicon elastomer to ~12 at 400 MHz, while maintaining the tanδ at ~0.05 [36]. Wang et al. used poly(vinyl alcohol)-modified RGO as the filler materials for PVDF [37]. The resultant composite displayed $\varepsilon'$ value of ~230 at 2.2 vol.% filler content. The dielectric loss of the composite, however, was not provided. Fan et al. reported that 0.177 vol.% RGO loading improves dielectric permittivity of PVDF to more than 150 at 1 kHz [38]. Nevertheless, the loss tangent approached 1, thereby limiting the potential applications of such a composite. Romasanta et al. observed a low dielectric permittivity of less than 15 at 1 kHz in polydimethylsiloxane (PDMS) filled with 2 wt.% TRG. The dielectric loss at such filler content is as low as 0.03 [39]. They attributed the low loss tangent to the remnant oxygen functional groups on the RGO, which are beneficial in achieving low dielectric loss while maintaining a reasonable high dielectric permittivity.

For practical application of a material in dielectric capacitors, a low electrical conductivity is required in order to prevent the electrical charge flow from one electrode plate to another. Figure 6 shows that the electrical conductivity of the Ag-RGO/PVDF composite rises almost linearly with increasing frequency, even at a 1.5 vol.% filler content. This indicates a good insulating property for the composite below $p_c$. The suppressed electrical conductivity, as well as the significantly increased dielectric permittivity and decreased dielectric loss achieved in the composite, strongly showing that the Ag-RGO sheets are very

effective fillers for improving the dielectric performance of the polymers.

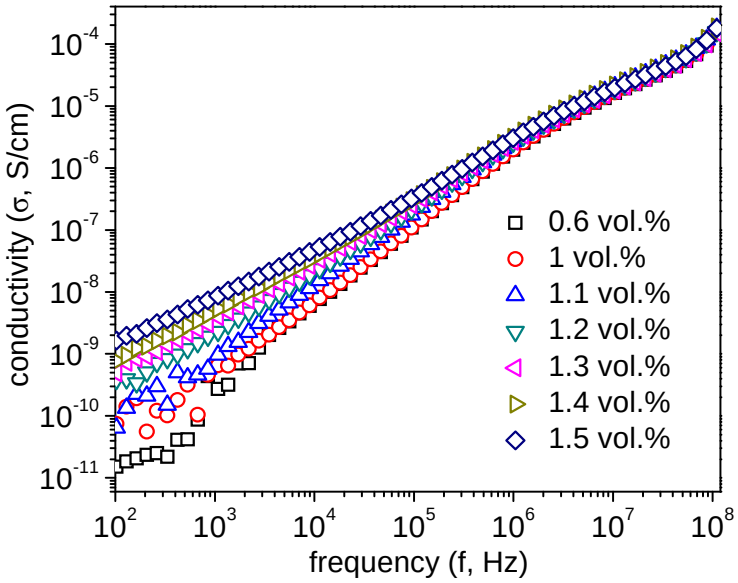


Figure 6 Frequency-dependent electrical conductivity of Ag-RGO/PVDF composites.

## 4. Conclusions

In this study, Ag-RGO sheets were prepared and used as nanofillers for fabricating Ag-RGO/PVDF composites. Near the percolation threshold ($p$ = 1.52 vol.%), the composite system shows a ten-fold increase in dielectric permittivity, which reaches a value of about 97 at 1 kHz, while maintaining a relatively low dielectric loss. It is considered that the Ag nanoparticles anchored on the RGO sheets can prevent these sheets from aggregation, resulting in large increase of interfacial areas within the composites. When exposed to external electric field, the increased interfacial areas produce Maxwell−Wagner−Sillars effect, leading to an enhancement in dielectric permittivity. In addition, the composites below $p_c$ exhibited a relatively low electrical conductivity, rendering them ideal dielectric materials for electronic capacitor applications.

**Acknowledgments**

This work was funded by King Abdulaziz University, under grant no. (9-130-1434-HiCi). The authors, therefore, acknowledged financial support of KAU.

References

[1] S. C. Tjong, S. L. Liu and R.K.Y. Li, *J. Mater. Sci.* 1996, **31**, 479-484

[2] J. Z. Liang, R. K. Y. Li and S. C. Tjong, *Polym. Compos.*, 1999, **20**, 413-422.

[3] S. C. Tjong and Y. Z. Meng, *Polymer*, 1997, **38**, 4609-4615.

[4] K.L. Fung, R. K. Y. Li and S. C. Tjong, *J. Appl. Polym. Sci*., 2002, **85**, 169-176.

[5] Z. M. Dang, J. K. Yuan, J. W. Zha, T. Zhou, S. T. Li and G. H. Hu, *Prog. Mater. Sci.*, 2012, **57**, 660-723.

[6] Z. M. Dang, B. Peng, D. Xie, S. H. Yao, M. J. Jiang and J. Bai, *Appl. Phys. Lett.*, 2008, **92**, 112910.

[7] Z. M. Dang, Y. H. Zhang and S. C. Tjong, *Synth. Met.*, 2004, **146**, 79-84.

[8] L. Qi, B. I. Lee, S. Chen, W. D. Samuels and G. J. Exarhos, *Adv. Mater.*, 2005, **17**, 1777–1782.

[9] S. P. Bao, G. D. Liang and S. C. Tjong, *Carbon*, 2011, **49**, 1758-1768.

[10] L. He and S. C. Tjong, *J. Nanosci. Nanotech.*, 2011, **11**, 10668–10672.

[11] L. He and S. C. Tjong, *Current Nanoscience*, 2010, **6**, .40-44.

[12] L. He and S. C. Tjong, *Synth. Met.*, 2012, **162**, 2277-2281

[13] http://www.nanoamor.com

[14] K. S. Novoselov, A. K. Geim, S. V. Morozov, D. Jiang, Y. Zhang, S. V. Dubonos, I. V. Grigorieva and A. A. Firsov, *Science*, 2004, **306**, 666-669.

[15] D. R. Dreyer, R. S. Ruoff and C. W. Bielawski, *Angew. Chem. Int. Ed.*, 2010, **49**, 9336-9344.

[16] S. Stankovich, D. A. Dikin, G. H. B. Dommett, K. M. Kohlhaas, E. J. Zimney, E. A. Stach, R. D. Piner, S. T. Nguyen and R. S. Ruoff, *Nature*, 2006, **442**, 282-286.

[17] X. Li, W. Cai, J. An, S. Kim, J. Nah, D. Yang, R. Piner, A. Velamakanni, I. Jung, E. Tutuc, S. K. Banerjee, L. Colombo and R. S. Ruoff, *Science*, 2009, **324**, 1312-1314.

[18] L. He and S. C. Tjong, *Nanoscale Res. Lett.*, 2013, **8**, 132.

[19] L. He and S. C. Tjong, *RSC Adv.*, 2013, **3**, 22981–22987.

[20] T. Kuilla, S. Bhadrab, D. Yao, N. H. Kim, S. Bose and J. H. Lee, *Prog. Polym. Sci.*, 2010, **35**, 1350-1375.

[21] S. Stankovich, D. A. Dikin, G. H. Dommett, K. M. Kohlhaas, E. J. Zimney, E. A. Stach, R. D. Piner, S. T. Nguyen and R. S. Ruoff, *Nature*, 2006, **442**, 282-285.

[22] J. Lu, K. S. Moon and C. P. Wong, *J. Mater. Chem.*, 2008, **18**, 4821–4826.

[23] J. Lu, K. S. Moon, J. Xu and C. P. Wong, *J. Mater. Chem.*, 2006, **16**, 1543–1548.

[24] H. S. Nalwa, *Ferroelectric Polymers: Chemistry, Physics and Applications.* Marcel Dekker, New York, 1995.

[25] W. S. Hummers and R. E. Offeman, *J. Am. Chem. Soc.*, 1958, **80**, 1339-1339.

[26] F. M. Du, J. E. Fischer and K. I. Winey, *J. Polymer. Sci.*, 2003, **41**, 3333-3338.

[27] C. W. Nan, Y. Shen and J. Ma, *Annu. Rev. Mater. Res.*, 2010, **40**, 131-151.

[28] C. W. Nan, *Prog. Mater. Sci.* 1993, **37**, 1-116.

[29] A. Javada, Y. Xiao, W. Xu, and S. Gong, *J. Mater. Chem.*, 2012, **22**, 830−834.

[30] L. Cui, X. Lu, D. Chao, H. Liu, Y. Li and C. Wang, *Phys. Status Solidi A*, 2011, **208**, 459−461.

[31] F. Wen, Z. Xu, S. Tan, W. Xia, X. Wei and Z. Zhang, *ACS Appl. Mater. Interfaces.*, 2013, **5**, 9411−9420.

[32] J. Shang, Y. Zhang, L. Yu, X. Luan, B. Shen, Z. Zhang, F. Lv and P. K. J. Chu, *Mater. Chem. A*, 2013, **1**, 884−890.

[33] D. Pan, S. Wang, B. Zhao, M. Wu, H. Zhang, Y. Wang and Z. Jiao, *Chem. Mater.*, 2009, **21**, 3136−3142.

[34] A. Moliton, *Applied Electromagnetism and Materials*. Springer, New York, 2007.

[35] J. Y. Kim, W. H. Lee, J. W. Suk, J. R. Potts, H. Chou, I. N. Kholmanov, R. D. Piner, J. Lee, D. Akinwande and R. S. Ruoff, *Adv. Mater.*, 2013, **25**, 2308–2313.

[36] A. Dimiev, W. Lu, K. Zeller, B. Crowgey, L. C. Kempel and J. M. Tour, *ACS Appl. Mater. Interfaces*, 2011, **3**, 4657–4661.

[37] D. Wang, Y. Bao, J. W. Zha, J. Zhao, Z. M. Dang and G. H. Hu, *ACS Appl. Mater. Interfaces*, 2012, **4**, 6273−6279.

[38] P. Fan, L. Wang, J. Yang, F. Chen and M. Zhong, *Nanotechnology*, 2012, **23**, 365702.

[39] L. J. Romasanta, M. Hernández, M. A. López-Manchado and R. Verdejo, *Nanoscale Res. Lett.*, 2011, **6**, 508.